Separation Science and Technology

ISSN: 0149-6395 (Print) 1520-5754 (Online) Journal homepage: https://www.tandfonline.com/loi/lsst20

Metal chelate based site recognition of ceruloplasmin using molecularly imprinted polymer/cryogel system

Ibrahim Dolak, Gurbet Canpolat, Arzu Ersöz & Rıdvan Say

To cite this article: Ibrahim Dolak, Gurbet Canpolat, Arzu Ersöz & Rıdvan Say (2019): Metal chelate based site recognition of ceruloplasmin using molecularly imprinted polymer/cryogel system, Separation Science and Technology, DOI: 10.1080/01496395.2019.1577446

To link to this article: https://doi.org/10.1080/01496395.2019.1577446

Published online: 22 Feb 2019.

SEPARATION SCIENCE AND TECHNOLOGY
https://doi.org/10.1080/01496395.2019.1577446

Metal chelate based site recognition of ceruloplasmin using molecularly imprinted polymer/cryogel system

Ibrahim Dolak[a], Gurbet Canpolat[b], Arzu Ersöz[c,d], and Rıdvan Say[e]

[a]Vocational School of Technical Sciences, Dicle University, Diyarbakır, Turkey; [b]Department of Chemistry, Siirt University, Siirt, Turkey; [c]Department of Chemistry, Eskişehir Technical University, Eskişehir, Turkey; [d]Bionkit Co Ltd., Eskişehir, Turkey; [e]Department of Chemistry, Anadolu University, Eskişehir, Turkey

ABSTRACT

In the present study, N-Acetylneuraminic acid (NANA)-imprinted poly(2-hydroxyethyl methacrylate-N-methacryloyl-(L)-histidin-Cu(II)) p(HEMA-(MAH)$_2$-Cu(II)) has been synthesized by radical polymerization for site recognition of ceruloplasmin. Prepared imprinted cryogel has been characterized by scanning electron microscopy (SEM) and Fourier transform infrared spectroscopy (FTIR). When the binding capacity of NANA-imprinted cryogel (MIP) was compared with non-imprinted cryogel (NIP), it was found that MIP has higher adsorption capacity. The maximum amount of binding NANA has found as 83.20 mgg^{-1} at pH 7.0 with flow rate of 1 mLmin^{-1} at 25°C. Selectivity experiments for MIP and NIP cryogel have been carried out via the NANA/D-mannose and ceruloplasmin/immunoglobulin G (IgG) pair separately and the relative selectivity coefficient (k′) has found as 77.46 and 17.97, respectively. Applicable of the MIP in human serum has been studied and resulted successfully.

ARTICLE HISTORY
Received 3 April 2018
Accepted 2 January 2019

KEYWORDS
Ceruloplasmin; NANA-imprinted cryogel; metal-chelate complex; p-hema-mah; selective separation

Introduction

Ceruloplasmin is one of the multicopper glycoprotein present in the a_2-globulin fraction with molecular weight of about 151.000. It is a major copper-carrying protein and about % 95 of copper in humans blood plasma is bound to ceruloplasmin. Ceruloplasmin contains hexoamine, hexose and neuraminic acid (NANA).[1] Despite having many functions[2], ceruloplasmin is well known to play an active role in the oxidation of various substrates such as aromatic amines, phenols[3]; while the interest in ferrous iron (Fe^{2+}) is much more than above substrates that it is termed as ferroxidase activity.[4] Ferric iron (Fe^{3+}) which results from ferroxidase reaction become available to incorporate into the transferrin receptor for transport of iron to other cells where it is required for cellular metabolism.[5] Ferroxidase activity also associated with antioxidant activity because that prevents the generation of superoxide and hydroxyl radical which are stimulated by highly toxic ferrous iron.[6] Lack of ceruloplasmin in blood, however, has been reported to lead to accumulation of both highly toxic ferrous iron and copper in cells especially in liver, brain, pancreas, retina that results in oxidative damage.[7] It is indicated that, ceruloplasmin utilized as a medicine, specifically, as a blood antioxidant.[8]

As in all biomolecules, the selective isolation and quantification of ceruloplasmin are significant demand toward understanding its function, potential application and diseases that associated with its lack. Various chromatographic methods such as ion-exchange chromatography, gel electrophoresis or combining of two or three general chromatography methods for purification and determination of ceruloplasmin were applied.[9–13] However, these techniques have significant limitations such as low load ability and poor separation. Unlike the classical methods, molecular imprinting technology is very promising to create highly specific and sensitive cavities onto polymer which has higher physical robustness and inertness toward acids, bases and organic solvents. In addition, they are less expensive to be synthesized and can be used several times at room temperature without losing the recognition capacity.[14,15]

Molecular imprinting is a new technique has been attracted the attention of researchers for effective recognition of chemical and biological molecules including aminoacids, proteins, enzymes, DNA, drugs, phenolic compounds and metals.[16–28] This technique allows selective and sensitive recognition of chosen template molecule by leaving artificial-imprinted cavities in a polymer matrix that provides high affinity to the template molecule.[29] To synthesize molecularly imprinted polymer (MIP), the

CONTACT Gurbet Canpolat gokalp.gurbet@gmail.com Department of Chemistry, Siirt University, Siirt, Turkey
Color versions of one or more of the figures in the article can be found online at www.tandfonline.com/lsst.

template molecule and functional monomers which can arrange around template are complexed interactively before polymerization. Then, the rigid polymer matrix is obtained by polymerization of formed pre-complex and cross-linker reagent. After removal of template molecule from the polymer with suitable elution agent, the cavities remaining in the polymer that are complementary in shape, size and chemical functionality to the template. Consequently, the resultant polymer is able to recognize and rebind selectively the template or other molecules that are chemically related to the template.[15,30]

There are generally three approaches for molecular imprinting according to the nature of the interactions between the imprinted molecule and the functional monomer: covalent molecular imprinting, noncovalent molecular imprinting (electrostatic interactions, dipole interactions, van der Waals or hydrogen bonding) and metal-coordinating (chelating) molecular imprinting.[31]

Metal-coordinating based recognition is a great potential area for MIP due to its easy pre-organization, high stability and higher strength than hydrogen bonds in the polar system.[32] In the metal coordination approach, metal ion, generally a transition metal ion, is employed as mediator that coordinates functional monomer and template molecule to create high specificity and fast binding in the imprint. In addition, by choosing appropriate metal ion, the binding strength can be adjusted. Effectiveness of metal chelating interaction on the recognition was indicated in many studies.[29]

Despite many advantages of MIP on selective separation of target the molecule, it is also associated with some significant drawbacks. Especially, when the target molecule is highly expensive and hazardous (e.g., toxic), the use of the target molecule itself as a template in preparing the imprinting polymer can be prohibitively expensive.[33] In addition, imprinting of large molecules studies is limited due to some difficulties (e.g., steric hindrance, complexity, conformational instability of large molecules). An alternative approach is presented that, a template can be selected as closely related to target instead of the whole target molecule to reduce these complications.[34–36]

In this study, selective recognition and separation of ceruloplasmin were studied through MIP based cryogenic trap. Unlike the whole target imprinting technique, ceruloplasmin (target) was not directly imprinted because of its large size and high cost. As a new approach, the target's specific group (NANA) was imprinted alternatively and the selective recognition function is thought to be provided through this group after removed from the polymer system. MIP was synthesized and described how pH, initial concentration, flow rate, temperature and ionic strength affect the binding capacity to investigate optimal conditions. Our study was terminated by evaluation of selectivity of the prepared column, preconcentration of ceruloplasmin in aqueous solution and determination in human blood serum.

Materials and methods

Reagents

N-Acetylneuraminic acid (NANA) (98%), D-mannose (≥99%), bovine ceruloplasmin (CAS Number: 9031–37-2) and immunoglobulin G (IgG) from bovine serum (≥95%) were purchased from Sigma-Aldrich (Steinheim, Germany). The functional monomer 2-Hydroxyethyl methacrylate (HEMA) (97%), crosslinker N-N-methylenbisacrilamid (MBAAm) (99%), polymerization initiators N,N,N,N-tetramethylene diamine (TEMED) (99%) and Ammonium Persulfate (APS) (≥98%) were also provided from Sigma-Aldrich (Steinheim, Germany). The functional monomer, N-methacryloyl-L-histidine (MAH) was synthesized according to previously published paper.[37] In pH studies, acetate buffer solutions CH_3COOH (Merck, 100%)-$NaCH_3COOH$ (Sigma-Aldrich, ≥99%) and phosphate buffer $NaH_2PO_4.2H_2O$ (Merck, CAS Number; 13472–35-0)-Na_2HPO_4 (Merck, CAS Number; 7558–79-4) were used in the required compositional range. $CuSO_4.5H_2O$, NaOH, Na_2CO_3, NaCI and Na_2SO_4 were all analytical grade and obtained from Merck A.G.

Apparatus

Watson Marlow, Sci Q 300 peristaltic pump was used in all experiments for adjusting the flow rate. The incubator, Binder brand, was used to carry out temperature controlled studies. Mettler Toledo pH meter was used to control of the medium pH. Quantitation of sugars and proteins was performed by Shimadzu UV-3600 UV-VIS-NIR Spectrophotometer. Samples were characterized with Fourier transform infrared spectroscopy (FTIR) and scanning electron microscopy (SEM) methods; FTIR measurements were analyzed on a Perkin Elmer Laser model 400 Spektrum; for SEM analysis, samples were coated with gold nano surface and carried out on FEI Quanta FEG-250 model instrument. The measurement of copper content was performed using the Perkin Elmer Optima 7000 DV-ICP-OES instrument. The deionized water used in the experiment was also purified by using Millipore Milli-Q Plus Ultra-Pure system.

Preparation of preorganized monomer $(MAH)_2$-Cu (II)-NANA

The metal-chelate preorganized monomer was synthesized with minor modification of the method reported in the literature.[17] For this purpose, MAH (148 mg) and $CuSO_4.5H_2O$ (125 mg) that was taken in the 2:1 ratio (m/m) were dissolved in 10 mL of deionized water and stirred magnetically at room temperature overnight. Afterwards; NANA (10 mg) as mediated template molecule was added into the solution and reaction was proceeded for an overnight to synthesize $(MAH)_2$-Cu(II)-NANA complex (Fig. 1).

Preparation of NANA-imprinted p(HEMA-$(MAH)_2$-Cu (II)) (MIP) and non-imprinted cryogel (NIP) composite cryogel

p(HEMA-$(MAH)_2$-Cu(II))-NANA) based MIP cryogel was prepared according to the procedure that was applied by Tamahkar et al.[38] with minor modifications: Firstly, 1.3 mL of HEMA and 1 mL of $(MAH)_2$-Cu(II)-NANA preorganized monomer were mixed and stirred magnetically in a 25 mL borosilicate glass beaker. For monomer cross-linking 0.25 g MBAAm in deionized water (5 mL) was added into monomer mixture and allowed the reaction stirring magnetically. The MIP-cryogel was prepared by free radical polymerization in the presence of APS and TEMED as a second step. After the addition of APS (20 mg), the reaction mixture was cooled in an ice bath and TEMED (50 µL) was added and mixed for 3 min. followed by poured into a plastic syringe (5 mL) and frozen at −18°C. The polymerization mixture in the syringe, which had been kept at −18°C for overnight, was then thawed to room temperature for 30 min. and washed with 50 mL deionized water. Finally, to remove of NANA from p (HEMA-MAH-Cu(II)) cryogel, 0.1 M Na_2CO_3 and NaOH mixture as eluation solution were pumped through column until no NANA was detected in the eluting solution. Hereby, selective binding site for ceruloplasmin recognition was obtained (Fig. 2). NIP was also prepared in the absence of NANA using the same polymerization procedure as described above. Prepared MIP and NIP composite polymers were stored in 0.02% sodium azide buffer at 4°C until use.

Binding studies

All binding experiments were carried out with three stages which were equilibration, loading, and elution. Briefly, the NANA solution which was kept constant at 0.5 $mgmL^{-1}$ in all studies was pumped through the 0.2 g of MIP which were equilibrated with an appropriate buffer solution. Finally the template was removed in each experiment using 0.1 M Na_2CO_3 and NaOH mixture. All measurements were spectrometrically carried out. The effect of various parameters such as pH (4.0–8.0), initial NANA concentration (0.5–2.0 $mg.mL^{-1}$), flow rate (1.0–

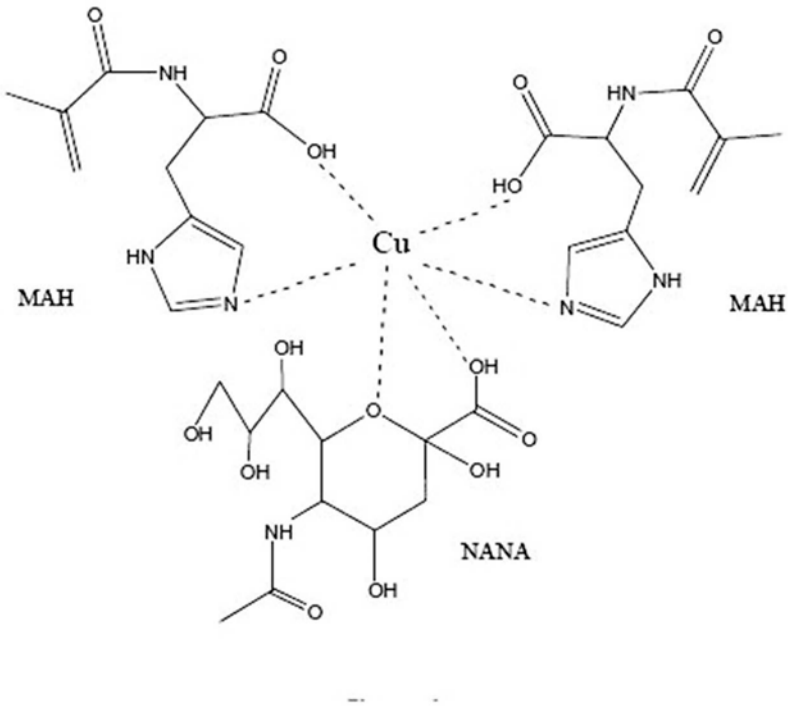

Figure 1. Schematic representation for $(MAH)_2$-Cu(II)-NANA preorganized monomer.

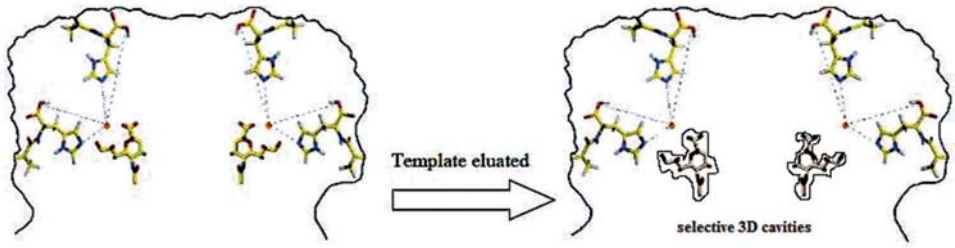

Figure 2. Schematic representation of NANA-imprinted polymer.

4.0 mLmin^{-1}), temperature (4–37°C) and ionic strength on binding capacity were investigated.

Characterization studies

The complex formation of MAH with Cu(II) was supported and MAH, $(MAH)_2Cu(II)$ and $(MAH)_2Cu(II)$-NANA complex were characterized by FT-IR. FT-IR and SEM were used for the characterization of NANA-MIP cryogel. The surface morphology of MIP cryogel was illustrated by SEM images. Swelling study of MIP cryogel polymer was carried out through; first, cryogel was dried and dry weight (m_d) was measured. Then, it was placed in a 30 mL vial containing distilled water and was allowed to swell until equilibrium swelling at 25°C for 2 h. The cryogel was removed from the vial, wiped by a filter paper and weighed of the swollen polymer (m_s). The swelling degree (S) was calculated by using the following equation:

$$S = \frac{m_s - m_d}{m_d}$$

For roughly determining the macroporous percentage (M%) of MIP cryogel, the swollen cryogel matrix was squeezed to remove free water and weighed ($m_{squeezed\ gel}$). M% was calculated according to;

$$M\% = \frac{m_s - m_{squeezed\ gel}}{m_s} \text{ x } 100$$

Results and discussion

Characterization of MAH, $(MAH)_2Cu(II)$, $(MAH)_2Cu(II)$-NANA preorganized monomer and NANA-imprinted p-HEMA-$(MAH)_2$-Cu(II) cryogel

From the FT-IR spectrum, the shifts in the double bond region were indicated from metal interactions and it is likely that the binding occurs in this region. Unlike the MAH and $(MAH)_2Cu(II)$, the wideband in the region of 3600–3000 cm^{-1} corresponds to OH stretching vibration of NANA structure. The band indicating that $(MAH)_2Cu(II)$ was included in the NANA template was observed at about 1100 cm^{-1} for C-O-C (ring ether) stretching vibrations. The amide bands as characteristic bands of the compounds arise at around 1600 cm^{-1}(Fig. 3a).

p(HEMA-$(MAH)_2$-Cu(II)) exhibited very similar FT-IR spectra with p-HEMA due to the similarity of the polymer backbone structure as seen in Fig. 3b. The equilibrium swelling degree and macroporosity of the NANA-imprinted p-HEMA-$(MAH)_2$-Cu(II) cryogel were 6.12 g H_2O/g cryogel and 81.04%, respectively. As seen in Fig. 3c, the cryogel had interconnected pores and the pore size was found as about 10 μm.

Effect of pH

Determination of optimum binding conditions was started with pH because of the high effect of pH on the binding. For this purpose, the binding of NANA onto MIP and NIP cryogels was studied both in acetate (pH: 4.0–5.0) and phosphate (pH: 6–8.0) buffers systems with time-dependent as shown in Fig. 4. The maximum amount of binding of NANA was achieved at pH 7.0 as 25.0 mgg^{-1} and 8.30 mgg^{-1} for MIP and NIP cryogels, respectively. The reason for lower binding at below and above pH 7.0 can be explained as follows: protonation of amine groups on MIP such as imidazole nitrogen in MAH might lead to decrease the ability of coordination with copper ion at low pH conditions. Otherwise, when pH was much higher than 7.0, the phosphate ions (HPO_4^{2-} and PO_4^{3-}) in buffer might compete with template NANA. A similar trend was reported in the literature.[39] From now on, pH 7 was used as optimum pH in all subsequent experiments.

Effect of flow rate

Figure 5 shows the amount of binding of NANA at different flow rates. For this experiment, flow rate values changed from 1 to 4 mLmin^{-1}. The results showed that the increase in flow rate through the column resulted in a decrease in the amount of bonded NANA from 25.0 to 22.60 mgg^{-1}. This can be explained by the insufficient interaction time of the mediated template molecule to bind to the cryogel pores at high flow rates. These results

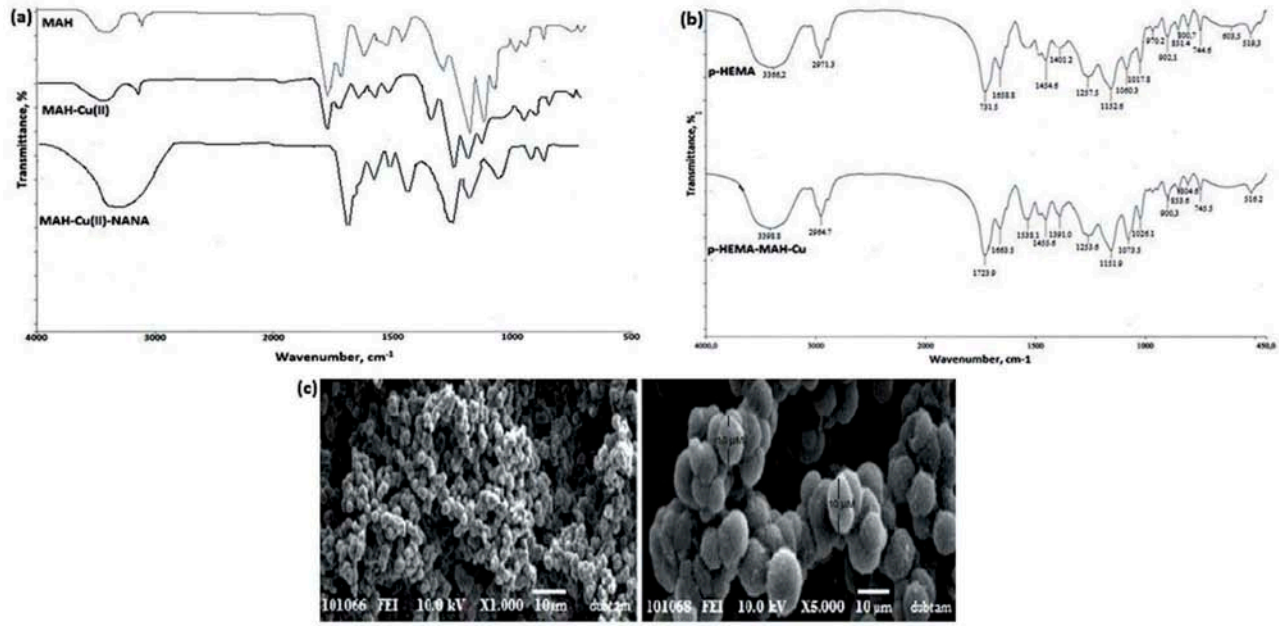

Figure 3. FT-IR Spectra of (a) MAH, Cu(II)$(MAH)_2$, Cu(II)$(MAH)_2$-NANA (b) p-HEMA and p(HEMA-$(MAH)_2$-Cu(II) cryogels (c) SEM images of NANA imprinted p(HEMA-$(MAH)_2$-Cu(II)) cryogel at a)1000x and b)5000x magnifications.

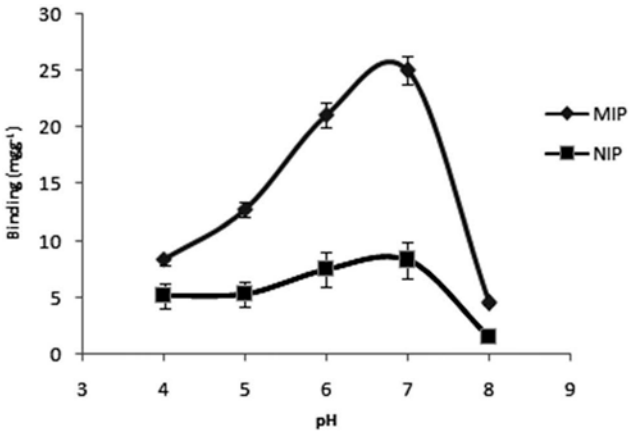

Figure 4. Effect of pH of binding on MIP and on NIP. Experimental conditions: Initial concentration: 0.5 $mgmL^{-1}$ in buffer, Flow rate:1 $mLmin^{-1}$, Temperature: 25°C.

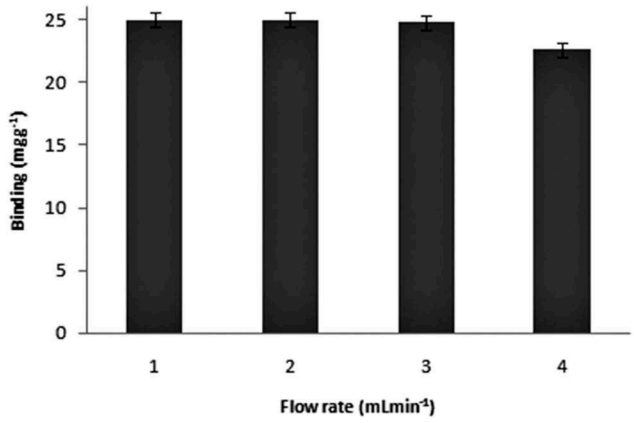

Figure 5. Effect of flow rate on binding. Experimental conditions: Initial concentration: 0.5 $mgmL^{-1}$, pH 7.0, Temperature: 25°C.

were in agreement with the refereed article.[18] Thus, 1 $mLmin^{-1}$ was selected as the optimum flow rate in the subsequent experiments.

Effect of initial concentration and evaluation of maximum binding capacity

The effect of the initial concentration which was considered the most effective parameter on binding capacity was studied between 0.5 to 2.0 $mgmL^{-1}$. As shown in Fig. 6, the amount of binding of NANA mediated increased linearly with increasing initial concentration. But for higher than 2 $mgmL^{-1}$ values, the rate of increase became insignificant that specified as saturation point. This is because at high concentration the binding sites of cryogel matrix become less and saturated. The maximum binding capacity was found to be 83.20 mgg^{-1} polymers within 2 h.

Effect of ionic strength

The effect of concentration and type of salt on binding capacity was investigated. For this purpose, the experiments were carried out between in 0.25 and 1.0 M NaCI and Na_2SO_4 salts. As shown in Fig. 7, when salt concentration increased from 0.25 to 1.0 M, the amount of binding of NANA decreased from 25.0 to 22.0 mgg^{-1} for

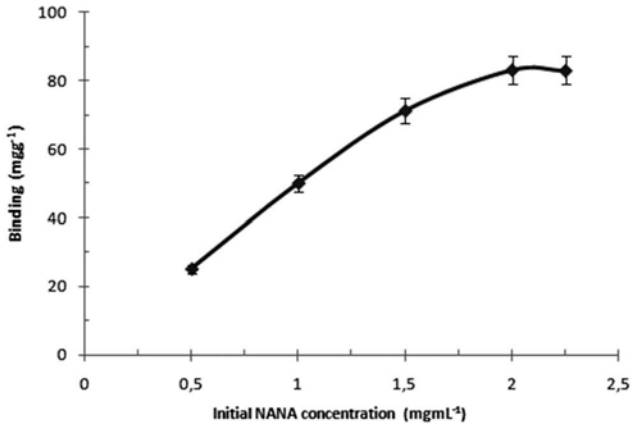

Figure 6. Effect of initial concentration. Experimental conditions: pH 7.0, Temperature: 25°C, 1.0 mLmin^{-1} flow rate.

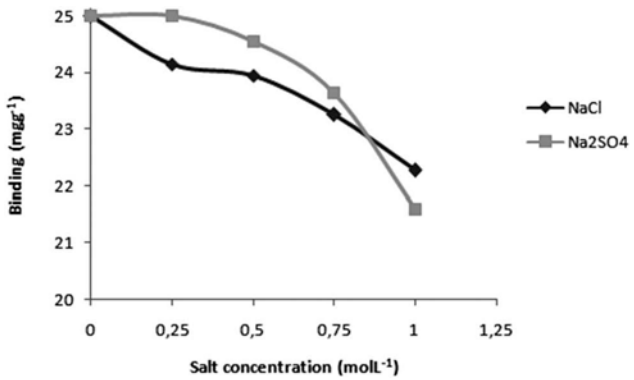

Figure 7. Effect of ionic strength of NaCl and Na_2SO_4 salts on binding. Experimental conditions: Initial concentration: 0.5 mgmL^{-1}; pH 7.0, Temperature: 25°C, 1.0 mLmin^{-1} flow rate.

each salt type similarly. This result suggested that ionic strength plays an important role on binding capacity that could explicable as following factors: (i) increasing of ionic strength would lead to decrease of noncovalent interactions (both hydrophobic and aromatic interactions) occurring between template and cryogel; (ii) the counter salt ions interact with the neuraminic acid via charge–charge interactions and mask the binding sites.[17]

Effect of the temperature

The determination of the effect of temperature on the binding capacity is also one the important parameter. Therefore, the effect of temperature on the binding of NANA was performed at 4, 25 and 37°C using Binder incubator. Experimental results showed that by increasing the temperature, the binding amount of template increased proportionally. However, when the temperature increased higher than 25°C, there was no continuous increase in bonded NANA and also a decrease was observed from 25.0 to 24.0 mgg^{-1}. This slight change can be explained that the increase in temperature can probably lead to conformational changes. Thus, it causes a decrease in the hydrophobic interaction between the template and MIP.

Reuse performans

The relationship between binding capacity and reuse performance of MIP cryogel was investigated at 11 binding–eluation cycles of NANA template. The elution of template from the MIP cryogel column was performed using 0.1 M Na_2CO_3 and NaOH mixture as the elution solution. The results as shown in Fig. 8, there was no difference in binding capacity that remained at around 100% even after 10 consecutive

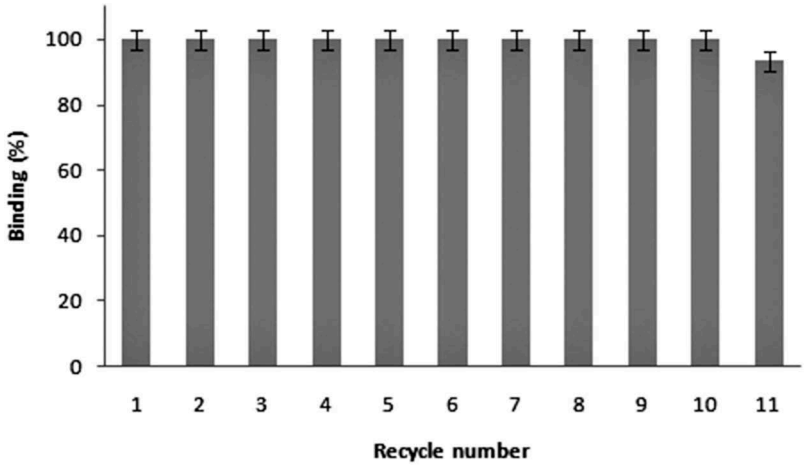

Figure 8. Reusability of MIP cryogel. Experimental conditions: Initial concentration: 0.5 mgmL^{-1}; pH 7.0, Temperature: 25°C, 1.0 mLmin^{-1} flow rate.

reuses. Thus, it was proved that the column remains stable during the experiments.

Selectivity experiments

Determination of the selectivity of NANA-imprinted polymer is one of the most critical experiments. Two paths were followed which are sugar-based and protein-based to study selectivity of NANA-imprinted p (HEMA-$(MAH)_2$-Cu(II)) cryogel.

For sugar-based selectivity (first path) (Fig. 9a), D-mannose was selected as an interfering competitive molecule. Mannose is a sugar found in the active region of many glycoproteins (e.g., IgG) and also is a hexose like NANA that becomes the reason for this selection. The binding amount of this interfering molecule onto the MIP was determined under optimal conditions which were determined experimentally as explained previously. Selectivity (k) of prepared column was determined as the ratio of the distribution constant (k_d) of the two compounds that was calculated according to follows:

$$k_d = \frac{C_i - C_e}{C_e} \times \frac{V}{m}$$

$$k = k_{d\ Template}/k_{d\ Interfering\ molecule}$$

where k_d is distribution constant (mLg^{-1}); k is the selectivity constant; C_i is initial compound concentration ($mgmL^{-1}$); C_e is the equilibrium compound concentration ($mgmL^{-1}$); V is volume of the solution (mL); m is the weight of the cryogel (g). The relative selectivity coefficient (k′) can be expressed:

$$k' = k_{MIP}/k_{NIP}$$

The result showed that the MIP has a high selectivity degree for the template with respect to the competitive compound (k_d for NANA is 292.46 and k_d = 11.27 for D-mannose) (Table 1). The selectivity constant of MIP for NANA was 25.95 times greater than D-mannose that proved cavities formed on the MIP cryogel were complementary in shape, size and chemical functionality to the template molecule, NANA. On the other hand, this value was found as 0.33 for the NIP column. It means that this column does not contain selective binding cavities.

Protein-based selectivity (Fig. 9b) study proved to bind of the target molecule ceruloplasmin protein too. In this respect, 2 mg ceruloplasmin and IgG were solved in 10 mL of phosphate buffer (pH 7.0) and then, the mixture was pumped through column under optimal conditions. As shown in Fig. 9b, binding amounts of proteins were found to be 9.12 mgg^{-1}cryogel and 2.07 mgg^{-1}cryogel for ceruloplasmin and IgG, respectively. The results showed that the selectivity constant (k) of MIP column for ceruloplasmin was 17.97 times greater than competitor protein IgG that was similar to sugar-based selectivity.

Application of prepared MIP on real sample

The importance of a study overlaps with its applicability to the real sample. To evaluate the applicability of the prepared cryogel, ceruloplasmin spiked blood serum was

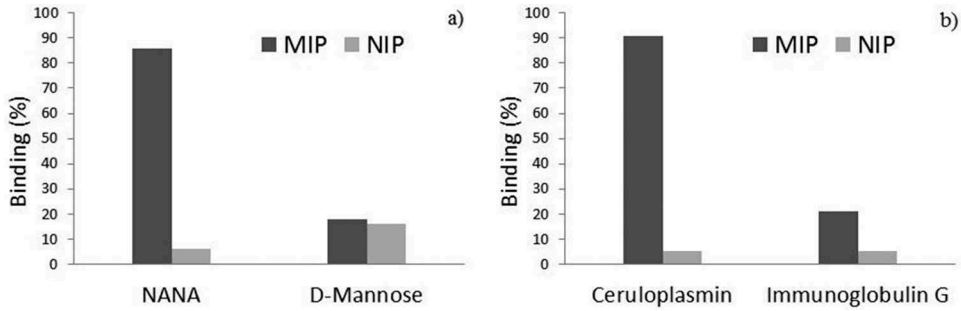

Figure 9. Sugar-based selectivity (a) and protein-based selectivity (b) of NANA-imprinted cryogel.

Table 1. Selectivity of NANA-MIP and NIP cryogel.

			MIP		NIP		
Molecule	Wavelength (nm)	Ci ($mgmL^{-1}$)	Ce ($mgmL^{-1}$)	k_D	Ce ($mgmL^{-1}$)	k_D	k′
NANA	420	0.5	0.07	292.46	0.47	3.19	77.46
D-Mannose	260	0.5	0.41	11.27	0.42	9.52	
Ceruloplasmin	409	0.2	0.02	505.55	0.19	2.63	17.97
IgG	511	0.2	0.16	28.12	0.19	2.63	

prepared as follows: blood sample taken from a healthy person was stored at +4°C. Then, it was centrifuged at 12000 rpmmin^{-1} for 15 min. to remove blood cells from plasma. Before the experiment, the serum sample was diluted to 1:2 using 5 mL of phosphate buffer (pH 7). Then, the concentration was adjusted to 50 ppm by adding 0.5 mg ceruloplasmin to this solution. Finally, serum solution containing ceruloplasmin was pumped through the column at a flow rate of 1.0 mLmin^{-1}, and then, eluted with 0.1 M Na_2CO_3 and NaOH mixture. The amount of ceruloplasmin in remaining (after binding) and elution solution was determined spectrometricallyat 409 nm as 3.71 and 45.12 ppm, respectively. It concluded that the binding capacity is 93.58% and the elution capacity is 96.43%.

Preconcentration of ceruloplasmin in aqueous solution

Preconcentration of samples with extremely low concentrations is an especially important step. With this approach, 250 mL of the aqueous solution containing 0.1 mgL^{-1} ceruloplasmin was pumped through the column at a flow rate of 1.0 mLmin^{-1} for 1 h for preconcentration of ceruloplasmin. Then, bonded ceruloplasmin was eluted from the polymer with 10 mL of 0.1 M Na_2CO_3 and NaOH mixture that the preconcentration factor resulted in 25. The concentration of ceruloplasmin in the elusion solution was found to be 2.48 mgL^{-1} with a binding capacity of 91.2% and could not be detected because the ceruloplasmin in the column outlet solution was below the LOD.

Conclusions

Low levels of ceruloplasmin induce free radical production and associated with Wilson's disease.[40] On the other hand, increased amounts are determined in active liver disease or tissue damage.[41] So it's important demand that purification and determination amount of ceruloplasmin to get information and to determine disease which associated with it. In this study, we designed site recognition of ceruloplasmin through N-Acetylneuraminic acid as the template and prepared NANA-imprinted p(HEMA-$(MAH)_2$-Cu(II)), unlike other classical imprinting technique. $(MAH)_2$Cu(II) as metal chelate functional comonomer was specifically selected due to a high binding capacity of ceruloplasmin to the copper metal that the reason for this choice was explained in the introduction section. After determination of optimum binding condition, the selectivity of the column was studied through on IgG besides D-mannose. The selectivity experiments proved that this method is tremendously selective for recognition of ceruloplasmin. It can be said that it is an important detection method in the diagnosis of ceruloplasmin-related diseases. The other advantages of technique can be listed as simple, low-cost, easy to apply and short process time. This is the first study for the selective site recognition of ceruloplasmin by molecular imprinting technique that will shed light on the recognition and separation of large and high-cost glycoproteins.

References

[1] Rıce, E.W.; Wagman, E.; Takenaka, Y. (1963) Ceruloplasmin assay in serum: standardization of ceruloplasmin activity in terms of international enzyme units. *Standard Methods of Clinical Chemistry*. 4: 39–46. doi:10.1016/b978-1-4831-9685-5.50012-1

[2] Osaki, S.; Walaas, O. (1967) Kinetic studies of ferrous ion oxidation with crystalline human ferroxidase. II. Rate constants at various steps and formation of a possible enzyme–substrate complex. *The Journal Of Bioloqical Chemistry*. 242: 2653–2657. PMID: 6027241.

[3] Wang, X.T.; Dumoulin, M.J.; Befani, O.; Mondovit, B.; Mateescu, M.A. (1994) Joint chromatographic purification of bovine serum ceruloplasmın and amineoxidase. *Preparative Biochemistry*. 24: 237–250. doi:10.1080/10826069408010096

[4] Erel, O. (1998) Automated measurement of serum ferroxidase activity. *Clinical Chemistry*. 44: 2313–2319. PMID: 9799759.

[5] The Medical Biochemistry Page, Iron and Copper Homeostasis. (2017) Retrieved from https://themedicalbiochemistrypage.org/iron-copper.php. (accessed 9 August 2017).

[6] Gutteridge, J.M. (1983) Antioxidant properties of caeruloplasmin towards iron- and copper-dependent oxygen radical formation. *FEBS Letters*. 157: 37–40. doi:10.1016/0014-5793(83)81111-9

[7] Collins, J.F.; Prohaska, J.R.; Knutson, M.D. (2010) Metabolic crossroads of iron and copper. *Nutrition Reviews*. 68: 133–147. doi:10.1111/j.1753-4887.2010.00271.x

[8] Sokolov, A.V.; Zakharova, E.T.; Shavlovskii, M.M.; Vasil'ev, V.B. (2005) Isolation of stable human ceruloplasmin and its interaction with salmon protamine. *Russian Journal of Bioorganic Chemistry*. 31: 238–248. doi:10.1007/s11171-005-0033-5

[9] Segelmark, M.; Persson, B.; Hellmark, T.; Wieslander, J. (1997) Binding and inhibition of myeloperoxidase (MPO): A major function of ceruloplasmin? *Clinical and Experimental Immunology*. 108: 167–174. doi:10.1046/j.1365-2249.1997.d01-992.x

[10] Calabrese, L.; Malatesta, F.; Barra, D. (1981) Purification and properties of bovine caeruloplasmin. *The Biochemical Journal*. 199: 667–673. doi:10.1042/bj1990667

[11] Killander, J. (1964) Separation of human heme- and hemoglobin-binding plasma proteins, ceruloplasmin and albumin by gel filtration. *Biochimica Et*

Biophysica Acta (BBA) General Subjects. 93: 1–14. doi:10.1016/0304-4165(64)90254-5

[12] Fuentes, P.; Gutiérrez, A.M.; Soler, L.; Cerón, J.J.; Martínez-Subiela, S. (2011) Development of fast and simple methods for porcine haptoglobin and ceruloplasmin purification. *Annales Veterinaria Murcia*. 26: 43–54.

[13] Ehrenwald, E.; Fox, P.L. (1994) Isolation of nonlabile human ceruloplasmin by chromatographic removal of a plasma metalloproteinase. *Archives of Biochemistry and Biophysics*. 309: 392–395. doi:10.1006/abbi.1994.1129

[14] Ertürk, G.; Mattiasson, B. (2017) Molecular imprinting techniques used for the preparation of biosensors. *Sensors*. 17: 288. doi:10.3390/s17020288

[15] Vasapollo, G.; Sole, R.D.; Mergola, L.; Lazzoi, M.R.; Scardino, A.; Scorrano, S.; Mele, G. (2011) Molecularly imprinted polymers: present and future prospective. *International Journal of Molecular Sciences*. 12: 5908–5945. doi:10.3390/ijms12095908

[16] Özcan, A.A.; Say, R.; Denizli, A.; Ersöz, A. (2006) L-Histidine imprinted synthetic receptor for biochromatography Applications. *Analytical Chemistry*, 78: 7253–7258. doi:10.1021/ac060536

[17] Çavuş, A.; Baysal, Z.; Alkan, H. (2013) Preparation of poly(hydroxyethyl methacrylate) cryogels containing L-histidine for insulin recognition. *Colloids and Surfaces. B, Biointerfaces*. 107: 84–89. doi:10.1016/j.colsurfb.2013.01.075

[18] Baysal, Z.; Aksoy, E.; Dolak, İ.; Ersöz, A.; Say, R. (2017) Adsorption behaviours of lysozyme onto poly-hydroxyethyl methacrylate cryogels containing methacryloyl antipyrine-Ce(III). *International Journal of Polymeric Materials and Polymeric Biomaterials*, 67: 199–204. doi:10.1080/00914037.2017.1320655

[19] Emir Diltemiz, S.; Denizli, A.; Ersöz, A.; Say, R. (2008) Molecularly imprinted ligand-exchange recognition assay of DNA by SPR system using guanosine and guanine recognition sites of DNA. *Sensors and Actuators B: Chemical,* 133: 484–488. doi:10.1016/j.snb.2008.03.007

[20] Bajpai, S.K.; Jhariya, S. (2016) Selective removal of amikacin from simulated polluted water using molecularly imprinting polymer: A column study. *Journal of Macromolecular Science, Part A: Pure and Applied Chemistry*. 53: 579–584. doi:10.1080/10601325.2016.1201754

[21] Dolak, İ.; Keçili, R.; Onat, R.; Ziyadanoğulları, B.; Ersöz, A.; Say, R. (2018) Molecularly imprinted affinity cryogels for the selective recognition of myoglobin in blood serum. *Journal of Molecular Structure*, 1174: 171–176. doi:10.1016/j.molstruc.2018.03.126

[22] Say, R.; Ersöz, A.; Atılır, A.; Diltemiz, S.; Denizli, A. (2005) Comparison of adsorption and selectivity characteristics for 4-nitrophenol imprinted polymers prepared via bulk and suspension polymerization. *Separation Science and Technology*. 39: 3471–3484. doi:10.1081/SS-200028939

[23] Dolak, İ. (2018) Selective separation and preconcentration of Thorium(IV) in bastnaesite ore using Thorium (IV)-Imprinted cryogel polymer. *Hacettepe Journal of Biology and Chemistry*, 46: 187–197. doi:10.15671/HJBC.2018.228

[24] Say, R.; Ersöz, A.; Denizli, A. (2003) Selective separation of uranium containing glutamic acid molecular-imprinted polymeric microbeads. *Separation Science and Technology*. 38: 3431–3447. doi:10.1081/ss-120023407

[25] Cankara, S.; Özkütük, E.B.; Öztürk, Ö.; Ersöz, A.; Say, R. (2016) Biopolymer based ion imprinting cryogel traps for the removal of Tl (I). *Separation Science and Technology*. 51: 901–908. doi:10.1080/01496395.2015.1105265

[26] Denizli, A.; Say, R.; Patir, S.; Arica, Y. (2001) Heavy metal separation capacity of a porous methacrylamidophenylalanine containing membrane based on a polyhydroxy-ethyl methacrylate matrix. *Separation Science and Technology*. 36: 2213–2231. doi:10.1081/ss-100105914

[27] Keçili, R.; Dolak, İ.; Ziyadanoğulları, B.; Ersöz, A.; Say, R. (2018) Ion imprinted cryogel-based supermacroporous traps for selective separation of cerium(III) in real samples. *Journal of Rare Earths*, 36: 857–862. doi:10.1016/j.jre.2018.02.008

[28] Dolak, İ.; Keçili, R.; Hür, D.; Ersöz, A.; Say, R. (2015) Ion-imprinted polymers for selective recognition of Neodymium(III) in environmental samples. *Industrial and Engineering Chemistry Research*, 54: 5328–5335. doi:10.1021/acs.iecr.5b00212

[29] Tamahkar, E.; Denizli, A. (2014) Metal ion coordination interactions for biomolecule recognition: a review. *Hittite Journal of Science and Engineering*. 1: 21–26. doi:10.17350/HJSE19030000004

[30] Saylan, Y.; Yilmaz, F.; Özgür, E.; Derazshamshir, A.; Yavuz, H.; Denizli, A. (2017) Molecular imprinting of macromolecules for sensor applications. *Sensors*. 17: 898. doi:10.3390/s17040898

[31] Ge, Y.; Turner, A.P.F. (2008) Too large to fit? Recent developments in macromolecular imprinting. *Trends in Biotechnology*. 26: 218–224. doi:10.1016/j.tibtech.2008.01.001

[32] Matsui, J.; Nicholls, I.A.; Takeuchi, T.; Mosbach, K.; Karube, I. (1996) Metal ion mediated recognition in molecularly imprinted polymers. *Analytica Chimica Acta*. 335: 71–77. doi:10.1016/s0003-2670(96)00356-x

[33] Gluckman, J.P.; Southard, G.E. (2016) Molecularly imprinted polymer beads for extraction of metals and uses thereof. Patent Number US9504988.

[34] Rachkov, A.; Minoura, N. (2000) Recognition of oxytocin and oxytocin-related peptides in aqueous media using a molecularly imprinted polymer synthesized by the epitope approach. *Journal of Chromatography A*. 889: 111–118. doi:10.1016/s0021-9673(00)00568-9

[35] Diltemiz, S.E.; Say, R.; Büyüktiryaki, S.; Hür, D.; Denizli, A.; Ersöz, A. (2008) Quantum dot nanocrystals having guanosine imprinted nanoshell for DNA recognition. *Talanta*. 75: 890–896. doi:10.1016/j.talanta.2007.12.036

[36] Büyüktiryaki, S.; Say, R.; Denizli, A.; Ersöz, A. (2017) Phosphoserine imprinted nanosensor for detection of cancer antigen 125. *Talanta*. 167: 172–180. doi:10.1016/j.talanta.2017.01.093

[37] Hür, D.; Ekti, S.F.; Say, R. (2007) N-Acylbenzotriazole mediated synthesis of some methacrylamido amino acids. *Letters in Organic Chemistry*. 4: 585–587. doi:10.2174/157017807782795556

[38] Tamahkar, E.; Bereli, N.; Say, R.; Denizli, A. (2011) Molecularly imprinted supermacroporous cryogels for cytochrome c recognition. *Journal of Separation Science*. 34: 3433–3440. doi:10.1002/jssc.201100623

[39] Xi, F.; Wu, J. (2004) Macroporous chitosan layer coated on non-porous silica gel as a support for metal chelate affinity chromatographic adsorbent. *Journal of Chromatography A*. 1057: 41–47. doi:10.1016/j.chroma.2004.09.059

[40] Kodama, H.; Fujisawa, C.; Bhadhprasit, W. (2012) Inherited copper transport disorders: biochemical mechanisms, diagnosis, and treatment. *Current Drug Metabolism*. 13: 237–250. doi:10.2174/138920012799320455

[41] Dominiczak, M.H.; Fraser, W.D. (2014) Blood and plasma proteins, In: Baynes, J.W.; Dominiczak, M.H. editors. *Medical Biochemistry: With Student Consult, Saunders*. 4th ed, 31–39; US: Academic Press..